

The Lupus-Associated Fc γ Receptor IIb–I232T Polymorphism Results in Impairment in the Negative Selection of Low-Affinity Germinal Center B Cells Via c-Abl in Mice

Jyun-Pei Zhou, I-Shing Yu, Haw Hwai, Chih-Shan Chen,
Pei-Lung Chen, and Shiang-Jong Tzeng

Objective. Fc γ receptor IIb (Fc γ RIIb) is an essential negative regulator of B cells that blocks B cell receptor (BCR) signaling and triggers c-Abl–dependent apoptosis of B cells. Fc γ RIIb-deficient mice display splenomegaly with expansion of B cells, leading to lupus. Fc γ RIIb-I232T is a hypofunctional polymorphism associated with lupus susceptibility in humans, an autoimmune disease linked to diminished deletion of autoreactive B cells. In the context of the Fc γ RIIb-I232T polymorphism, we investigated the role of Fc γ RIIb in the deletion of low-affinity germinal center (GC) B cells, an important mechanism for preventing autoimmunity.

Methods. We generated Fc γ RIIb^{232T/T} mice to mimic human Fc γ RIIb-I232T carriers and immunized mice with chicken gamma globulin (CGG)–conjugated NP, a T cell–dependent antigen, to examine the response of GC B cells.

Results. Compared to wild-type (WT) mice, Fc γ RIIb^{232T/T} mice showed increased numbers of low-affinity NP-specific IgG and NP-specific B cells and plasma cells; additionally, the expression of a somatic mutation (W33L) in their V_H186.2 genes encoding high-affinity BCR was reduced. Notably, Fc γ RIIb^{232T/T} mice had a higher number of GC light zone B cells and showed less apoptosis than WT mice, despite having equivalent follicular helper T cell numbers and function. Moreover, phosphorylation of c-Abl was reduced in Fc γ RIIb^{232T/T} mice, and treatment of WT mice with the c-Abl inhibitor nilotinib during the peak of GC response resulted in reduced affinity maturation reminiscent of Fc γ RIIb^{232T/T} mice.

Conclusion. Our findings provide evidence of a critical role of Fc γ RIIb/c-Abl in the negative selection of GC B cells in Fc γ RIIb^{232T/T} mice. Importantly, our findings indicate potential benefits of up-regulating Fc γ RIIb expression in B cells for treatment of systemic lupus erythematosus.

Fc γ receptor IIb (Fc γ RIIb) is a low-affinity Fc γ receptor for IgG. The Fc portion of IgG binds to the second Ig domain located near the transmembrane region of Fc γ RIIb proteins (1,2). In B cells, Fc γ RIIb is an indispensable inhibitory regulator. Fc γ RIIb-deficient mice exhibit splenomegaly due to expansion of B cells and eventually develop lupus-like disease (3,4). Depending on the affinity of antigens to the B cell receptor (BCR), Fc γ RIIb can transduce 2 distinct inhibitory signals upon stimulation of IgG immune complexes (ICs) to block B cell function (5). When Fc γ RIIb is co-ligated to the BCR, Fc γ RIIb blocks BCR signaling for proliferation and differentiation, and when independently engaged, Fc γ RIIb triggers B cell apoptosis by a c-Abl–dependent mechanism (1,2,5). When the BCR and Fc γ RIIb are co-engaged, the cytoplasmic immunoreceptor tyrosine-based inhibition motif of Fc γ RIIb is phosphorylated by the Lyn kinase, followed by recruitment of the lipid phosphatase SH2 domain–containing inositol-5'-phosphatase (SHIP), which hydrolyzes PI(3–5)P₃ to antagonize phosphatidylinositol 3-kinase signals for activation and proliferation of B cells (6–8). On the other hand, when the antigen in IgG ICs has low or no affinity for BCRs, Fc γ RIIb can directly trigger apoptosis of B cells via c-Abl kinase (5). The Fc γ RIIb-dependent apoptosis of B cells has been proposed to play a role in the elimination of autoreactive B cells, which emerge as low-affinity B cells in the germinal center (GC) (9), but evidence from in vivo studies is largely lacking.

The human Fc γ RIIb-I232T polymorphic variant, in which the isoleucine at position 232 of Fc γ RIIb is

Supported by the Ministry of Science and Technology of the Executive Yuan of Taiwan (grant NSC99-2320-B-002-011).

Jyun-Pei Zhou, MS, I-Shing Yu, PhD, Haw Hwai, MD, Chih-Shan Chen, MS, Pei-Lung Chen, MD, PhD, Shiang-Jong Tzeng, MD, PhD: National Taiwan University, Taipei, Taiwan.

Address correspondence to Shiang-Jong Tzeng, MD, PhD, Graduate Institute of Pharmacology, National Taiwan University, Taipei 10051, Taiwan. E-mail: sjtzeng@ntu.edu.tw.

Submitted for publication August 14, 2017; accepted in revised form May 8, 2018.

replaced by threonine, is a risk allele for systemic lupus erythematosus (SLE). The prevalence of Fc γ RIIb-I232T carriers has been reported to be up to 40% of SLE patients in Africans and Southeast Asians (10–12). Biochemical and imaging analyses have revealed a decreased association of Fc γ RIIb-232T proteins with lipid microdomains on the plasma membranes, resulting in blocking the association with BCR that results in inhibitory signaling (13–15). Nevertheless, people carrying the Fc γ RIIb-232T allele are protected against malaria infection owing to enhanced antibody response (12,16,17). Conversely, these subjects are susceptible to autoimmune diseases, e.g., SLE (12). Consistent with these findings, the surface expression of wild-type (WT) Fc γ RIIb in memory B cells and plasma cells (PCs) is down-regulated in patients with SLE (18–20). Furthermore, a failure to up-regulate Fc γ RIIb expression on GC B cells has been found in lupus-prone mice regardless of their genetic background (21). These findings strongly suggest a role of Fc γ RIIb in the GC response and raise the question of whether the hypofunctional Fc γ RIIb-232T allele might result in abnormality in the clonal selection of B cells in GCs, particularly in the deletion of low-affinity autoreactive B cells.

The GC is a critical site for antigen-driven selection of GC B cells for differentiation into PCs to generate high-affinity antibodies for protective immunity. In response to antigen, GC B cells first undergo V(D)J gene hypermutation of their BCRs in the dark zone, followed by migration of GC B cells to the adjacent light zone for selection of cells with high affinity to antigen, a critical process known as affinity maturation (22–24). Importantly, while high-affinity GC B cells are positively selected for further development into memory B cells and PCs, GC B cells carrying mutated BCRs of low or no antigenic affinity are negatively selected for apoptosis (25,26). To investigate the pathogenesis of human lupus associated with the Fc γ RIIb-I232T polymorphism, we generated Fc γ RIIb^{232T/T} mice to mimic human Fc γ RIIb-I232T carriers. Given that IgG ICs are readily formed after secondary immunization (27,28), the surface expression level of Fc γ RIIb in GC B cells is up-regulated (21), and Fc γ RIIb activation can trigger apoptosis of B cells via c-Abl (5), we reasoned that the Fc γ RIIb-232T allele with reduced inhibitory function might result in abnormal negative selection of GC B cells. Whether the dysfunction of the Fc γ RIIb-I232T polymorphism is linked to a GC defect is virtually unexplored. In addition, the consequences of abnormal GC reaction in the pathogenesis of autoimmune diseases are incompletely understood. Importantly, new insights into the causal relationship between the Fc γ RIIb-I232T polymorphism and the pathogenesis of SLE may provide valuable implications

for therapeutic exploitation of Fc γ RIIb for patients with SLE and perhaps other autoimmune diseases.

MATERIALS AND METHODS

Reagents. Chicken gamma globulin-conjugated NP₂₀ (NP₂₀-CGG), bovine serum albumin (BSA)-conjugated NP₇, BSA-conjugated NP₃₀, and phycoerythrin (PE)-conjugated NP were purchased from LGC Biosearch Technologies. Imject Alum adjuvant was acquired from Thermo Scientific. F(ab')₂ goat anti-mouse IgG and IgM antibodies were purchased from Jackson ImmunoResearch. Mouse IgG isotypes and monoclonal antibodies (mAb) specific for CD16/32 (clone 2.4G2), PE-Cy7-conjugated CD19 (clone 1D3), BV421-conjugated CD138 (clone 281-2), PerCP-Cy5.5-conjugated CD11b (clone M1/70), Alexa Fluor 700-conjugated CD11c (clone HL3), and fluorescein isothiocyanate (FITC)-conjugated inducible costimulator (ICOS) (clone 7E.17G9) were purchased from BioLegend. Allophycocyanin (APC)-Cy7-conjugated B220 (clone RA3-6B2), BV605-conjugated CD86 (clone GL1), Alexa Fluor 647-conjugated GL-7 (clone GL-7), BV421-conjugated CXCR4 (clone 2B11), PE-Cy7-conjugated CD95 (clone Jo2), Alexa Fluor 647-conjugated CD4 (clone RM4-5), BV421-conjugated programmed death 1 (PD-1; clone J43), PE-conjugated CXCR5 (clone 2G8), and 7-aminoactinomycin D (7-AAD) were acquired from BD Biosciences. Ninety-six-well MultiScreen-HTS filter plates were acquired from Merck Millipore. Blood lancets were obtained from MEDpoint. Mouse reference serum was acquired from Bethyl Laboratories. Vectastain ABC kits containing biotinylated goat anti-rabbit IgG and rabbit anti-goat IgG mAb were purchased from Vector. Horseradish peroxidase (HRP)-conjugated isotype IgG and polyclonal antibodies specific to phospho-c-Abl (Y245) were obtained from Santa Cruz Biotechnology. The active caspase 3 mAb was purchased from Cell Signaling Technology. Nilotinib and DMSO were obtained from Selleckchem.

Fc γ RIIb^{232T/T} mice and immunization protocols. Fc γ RIIb^{232T/T} mice on a C57BL/6J background were generated at the gene knockout mouse core facility at the Center of Genomic Medicine of National Taiwan University (NTU). The ATT codon of isoleucine 231 in exon 5 of the *Fcgr2b* gene was mutated to ACT to encode threonine using a recombinering approach. A *neo* gene cassette flanked with *loxP* sequences was inserted into the intron 5 region. The targeting vector was then linearized for electroporation into JM8A3 embryonic stem cells (ESCs). Correctly targeted ESC clones were subsequently injected into C57BL/6 blastocysts to produce chimeras. Chimeric males were bred with C57BL/6 females to produce Fc γ RIIb^{232T/T} mice. To remove the *neo* cassette, Fc γ RIIb^{232T/T} mice were crossed with Sox2-Cre mice (Tg(Sox2-cre)1Amc/J), which were kindly provided by Dr. Ming-Ji Fann (National Yang-Ming University, Taipei, Taiwan). Male and female Fc γ RIIb^{232T/T} mice were bred to generate offspring carrying Fc γ RIIb^{232T/T} (WT), Fc γ RIIb^{232T/T} (heterozygote), or Fc γ RIIb^{232T/T} (homozygote) genotypes for experiments. All mice were maintained in specific pathogen-free conditions at the Center for Laboratory Animals in the College of Medicine of NTU. The protocols of animal use were reviewed, and the experiments were performed according to the guidelines approved by the Institutional Animal Care and Use Committee of the College of Medicine of NTU. Female mice (7–8 weeks old) were immunized with 50 μ g NP₂₀-CGG per mouse by

intraperitoneal injection. Nilotinib (2 mg/kg/day) was administered intraperitoneally once a day on days 7–9 after secondary immunization. Mice were killed the day after the last injection.

Flow cytometric analysis. Mouse splenocytes were stained with FITC-conjugated CD16/32 mAb for 10 minutes at 4°C, followed by addition of an antibody cocktail containing PE–Cy7–conjugated CD19, BV421-conjugated CD138, PerCP–Cy5.5–conjugated CD11b, Alexa Fluor 700–conjugated CD11c, Alexa Fluor 647–conjugated GL-7, and PE-conjugated NP for 20 minutes on ice. To distinguish GC light zone from dark zone B cells, mouse splenocytes were stained with FITC-conjugated CD16/32, APC–Cy7–conjugated B220, BV605-conjugated CD86, Alexa Fluor 647–conjugated GL-7, BV421-conjugated CXCR4, PE–Cy7–conjugated CD95, and PE-conjugated NP. Splenic follicular helper T (T_{fh}) cells were stained with the following mAb: APC–Cy7–conjugated B220, Alexa Fluor 647–conjugated CD4, BV421-conjugated PD-1, PE-conjugated CXCR5, FITC-conjugated ICOS, and BV605-conjugated CD69. Bone marrow cells were stained with FITC-conjugated CD16/CD32, BV421-conjugated CD138, PE–Cy7–conjugated CD19, PerCP–Cy5.5–conjugated CD11b, Alexa Fluor 700–conjugated CD11c, and PE-conjugated NP. Dead splenocytes and bone marrow cells were stained with 7-AAD for 5 minutes before being washed. Cells were processed for analysis using a multicolor LSRFortessa cytometer (BD Biosciences). Data were analyzed using FlowJo version 10.

Confocal microscopy. Splenic B cells from 8-week-old WT and FcγRIIb^{232T/T} mice were isolated (>98% purity) using a mouse B lymphocyte enrichment kit (catalog no. 557792; BD Biosciences) according to the manufacturer's instructions. Purified cells (2 × 10⁶/ml) were incubated with rabbit anti-mouse IgM (25 μg/ml) for 10 minutes on ice followed by Cy3-labeled goat anti-rabbit IgG (50 μg/ml) and FITC-labeled cholera toxin B (10 μg/ml), which binds the lipid raft resident protein ganglioside G_{M1}, for an additional 10 minutes. Cells were then placed on a shaker (200 revolutions per minute) and incubated at 25°C for the indicated times. After a brief wash, cells were immediately fixed with 4% paraformaldehyde for 10 minutes at room temperature before mounting on slides. Images were acquired, analyzed, and quantified using a Zeiss LSM 880 confocal microscope.

Enzyme-linked immunosorbent assay (ELISA). BSA-conjugated NP₇ or BSA-conjugated NP₃₀ (5 μg/ml) was added to 96-well high bind plates (100 μl/well; Corning) and incubated at 4°C overnight. Mouse serum samples were diluted to detect IgG (1:200,000) and IgM (1:15,000). After blocking and incubation at 4°C overnight, plates were washed, followed by addition of HRP-conjugated rabbit anti-mouse IgG (Fcγ-specific) (catalog no. 115-035-071; Jackson ImmunoResearch) or goat anti-mouse IgM (μ-specific) (catalog no. 115-035-075; Jackson ImmunoResearch) for a 1-hour incubation at room temperature. After washes, plates were developed with tetramethylbenzidine substrate and the reaction was quenched with 2N H₂SO₄. Plates were read at an optical density of 450 nm (OD_{450 nm}) and OD_{570 nm} using an ELISA plate reader (BioTek). The reading values of HRP activities were calculated using OD_{450 nm} minus OD_{570 nm}. Standard curves of IgM and IgG concentrations were generated using serially diluted samples of mouse reference serum.

Enzyme-linked immunospot (ELISpot) assay. ELISpot assay was performed as previously described (29,30), except that BSA-conjugated NP₇ and BSA-conjugated NP₃₀ were used as the immobilized antigens to capture NP-specific PCs. Briefly, HRP-conjugated goat anti-mouse IgG and IgM were

used for detection of PCs. Approximately 2 × 10⁴ cells/well and 1.6 × 10⁵ cells/well with 2-fold serial dilutions for the detection of IgG and IgM PCs, respectively, were incubated overnight at 37°C. Spots in wells were developed by addition of 50 μl per well of 3-amino-9-ethylcarbazole substrates and incubation for 30 minutes. After washes and complete air dry, plates were scanned to enumerate spots using a CTL S6 universal analyzer (Cellular Technology).

Immunohistochemical examination. Immunohistochemical analysis of mouse spleen sections was performed using standard procedures with Vectastain ABC kits. Deparaffinized sections (4 μm thick) were stained overnight at 4°C with antibodies specific to active caspase 3 or phospho-c-Abl according to the manufacturer's instructions. After washes with phosphate buffered saline (PBS)–Tween (PBS buffer with 0.1% [volume/volume] Tween 20), sections were incubated with a species-specific antibody conjugated with HRP for 1 hour at ambient temperature. Slides were washed thoroughly, followed by addition of 3,3'-diaminobenzidine substrates for development. Sections were counterstained with hematoxylin before mounting. Slides were photographed using an Axioplan 2 light microscope (Zeiss).

Sequence analysis of the V_H186.2 region of BCRs from NP+ GC B cells. Genomic DNA of sorted GC B cells (NP+B220+GL-7+IgG+; ~1,000 cells per mouse) was extracted using a QIAamp DNA micro kit (Qiagen). For the amplification of V_H186.2–J_H2 segments, 1 ng of genomic DNA was used as template, and polymerase chain reaction (PCR) products were generated from high-fidelity PrimeStar DNA polymerase (Takara Bio). The PCR primers have been described previously (31): forward primer, 5'-AGCTGTATCATGCTCTTCTTGGCA-3' and reverse primer, 5'-AGATGGAGGCCAGTGAGGGAC-3' (31). Illumina libraries were generated from PCR products using a TruSeq library preparation kit and were sequenced using Illumina MiSeq to generate paired-end reads of 300 nucleotides. Raw sequencing data were aligned to mouse germline V_H186.2 sequences using Burrows-Wheeler aligner and SAMtools (32,33). The W33L mutation percentages in first complementarity-determining region sequences were compared with those in WT mice.

Statistical analysis. Bar graphs were plotted and analyzed using GraphPad Prism software version 6.0. Student's unpaired *t*-test was used for statistical analysis. The *t*-test was modified by Welch's correction in case of unequal variance. Tukey's test with one-way analysis of variance was used to compare multiple groups. Results are presented as the mean ± SEM. *P* values less than 0.05 were considered significant.

RESULTS

FcγRIIb^{232T/T} mice exhibit enhanced antibody production with reduced affinity maturation. Because the isoleucine 232 residue of human FcγRIIb is conserved in mice (NCBI accession nos. NP_001070657.1 and NP_003992.3), we generated a mouse line, termed the FcγRIIb^{232T/T} mouse line, which carries a point mutation of the isoleucine residue at position 231 (232 in humans) replaced by threonine (Figure 1A). Consistent with previous findings of live cell imaging (15), the surface FcγRIIb-232T proteins and lipid rafts were neither stably

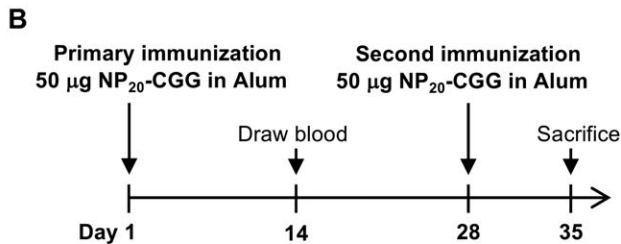
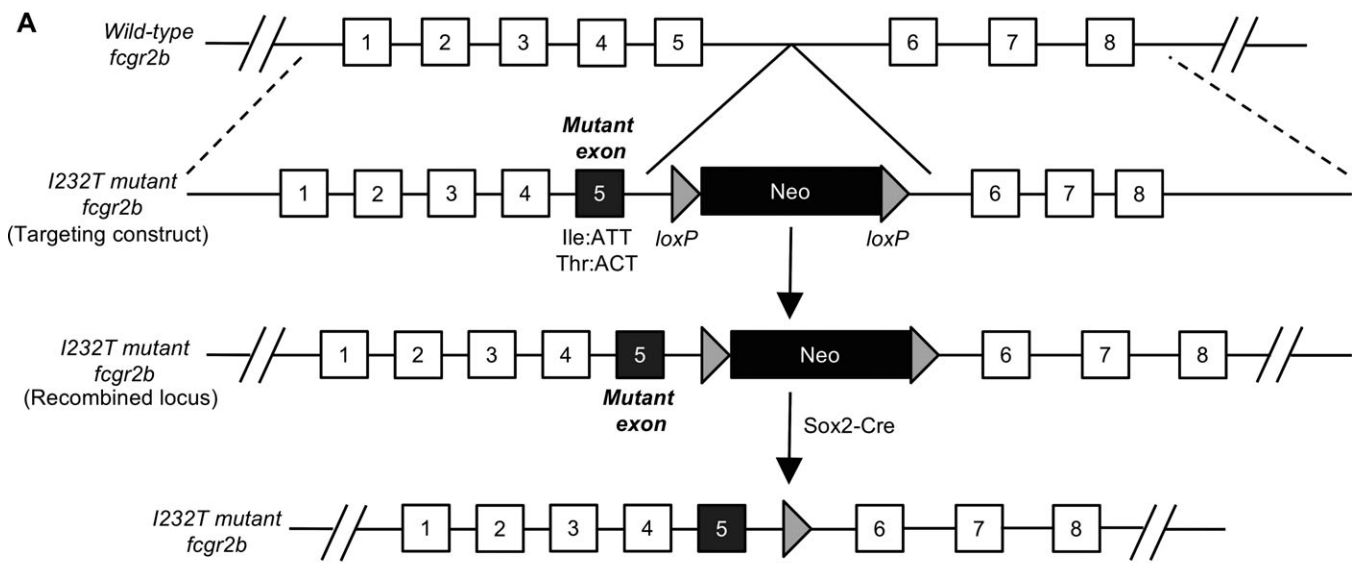


Figure 1. Generation of Fcγ receptor IIb (FcγRIIb)^{232T/T} mice and immunization schedule. **A**, Schematic diagram of the generation of FcγRIIb-I232T mutant mice. **B**, Schedule of immunization of mice with chicken gamma globulin-conjugated NP (NP₂₀-CGG). Wild-type and FcγRIIb^{232T/T} mice 7–8 weeks of age were each injected intraperitoneally with 50 μg of NP₂₀-CGG proteins mixed with 50 μl of alum. A second immunization was performed 4 weeks later.

associated nor co-clustered to form cap structures in splenic B cells (see Supplementary Figure 1, available on the *Arthritis & Rheumatology* web site at <http://onlinelibrary.wiley.com/doi/10.1002/art.40555/abstract>).

To investigate GC response, we immunized each WT and FcγRIIb^{232T/T} mouse by intraperitoneal injection with 50 μg of NP₂₀-CGG mixed with an equal volume of alum. All mice received a booster injection with the same amount of NP₂₀-CGG on day 28 after primary immunization and were killed on day 35, when clonal selection was actively proceeding (24,25) (Figure 1B). Serum samples were collected on day 14 and day 35 and tested in ELISA plates coated with either IgG-specific antibodies to detect total serum IgG, NP₃₀ to detect NP-specific antibodies of all affinities, or NP₇ to detect high-affinity NP-specific antibodies (30,31). The serum levels of total IgG were significantly higher in FcγRIIb^{232T/T} mice than in WT mice following both primary immunization (day 14) ($P = 0.0035$) and secondary immunization (day 35) ($P = 0.032$) (Figure 2A).

Fourteen days after the primary immunization, FcγRIIb^{232T/T} mice produced similar levels of high-affinity NP-specific antibodies ($P = 0.5033$) but more than double the amount of low-affinity NP-specific antibodies compared to WT mice ($P < 0.05$) (Figure 2B). By day 35, seven days after secondary immunization, FcγRIIb^{232T/T} mice produced significantly more high-affinity and low-affinity NP-specific antibodies than WT mice ($P < 0.05$ for NP₇; $P < 0.01$ for NP₃₀) (Figure 2B). The ratio of high-affinity to total (low affinity plus high affinity) NP-specific IgG (NP₇-bound IgG: NP₃₀-bound IgG) was lower in the serum of FcγRIIb^{232T/T} mice than in that of WT mice, indicating reduced affinity maturation of antibodies ($P < 0.05$) (Figure 2B). Moreover, sequencing of the NP-specific V_H186.2 region of B cells expressing NP-specific BCRs showed a decreased percentage of W33L replacement, which gives rise to high-affinity BCR variants, in FcγRIIb^{232T/T} mice ($P < 0.001$) (Figure 2C). In addition, we found a trend toward a lower ratio of replacement to silent hypermutation in FcγRIIb^{232T/T} mice

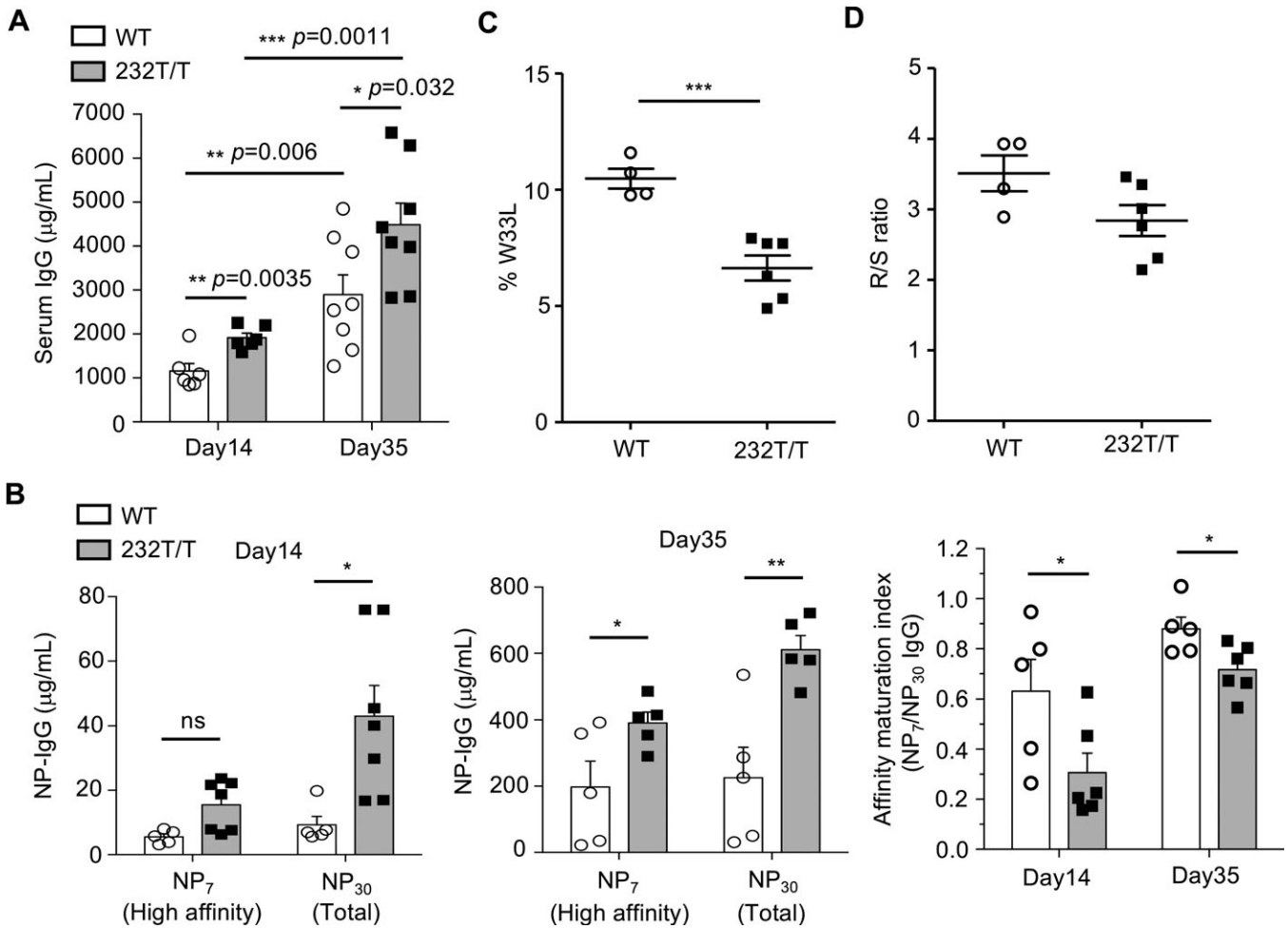


Figure 2. Enhanced NP-specific IgG production in immunized Fc γ receptor IIb (Fc γ RIIb)^{232T/T} mice. **A** and **B**, Serum levels of total IgG (**A**) and high-affinity NP₇ IgG and total NP₃₀ IgG (**B**) in wild-type (WT) mice and Fc γ RIIb^{232T/T} mice 2 weeks after primary immunization (day 14) ($P = 0.0035$ for IgG, $P = 0.5033$ for NP₇, and $P = 0.0469$ for NP₃₀) and 1 week after secondary immunization (day 35) ($P = 0.032$ for IgG, $P = 0.0411$ for NP₇, and $P = 0.0068$ for NP₃₀). In **B**, the ratios of NP₇ to NP₃₀ IgG levels in serum on day 14 ($P = 0.0427$) and day 35 ($P = 0.0277$) after immunization are also shown. Symbols represent individual mice; bars show the mean \pm SEM ($n = 5$ –8 mice per group). **C**, Frequency of W33L mutation in the V_H186.2 region of individual B cell receptor (BCR) genes of NP⁺ germinal center (GC) B cells in WT mice and Fc γ RIIb^{232T/T} mice 7–8 days after primary immunization ($P = 0.0008$). **D**, Ratio of replacement mutations to silent mutations (R:S) in the V_H186.2 region in NP⁺ GC B cells in WT mice and Fc γ RIIb^{232T/T} mice ($P = 0.0845$). In **C** and **D**, symbols represent individual mice; horizontal and vertical lines show the mean \pm SEM ($n = 4$ WT mice and 6 Fc γ RIIb^{232T/T} mice). * = $P < 0.05$; ** = $P < 0.01$; *** = $P < 0.001$. NS = not significant.

than in WT mice 8 days after primary immunization (Figure 2D). These results indicate a dysfunction in the affinity maturation of GC B cells in Fc γ RIIb^{232T/T} mice.

Retention of low-affinity B cells in Fc γ RIIb^{232T/T} mice after secondary immunization. Because affinity maturation was reduced in Fc γ RIIb^{232T/T} mice compared to WT mice, we investigated whether the elimination of low-affinity antigen-specific B cells was abnormal in GCs. As shown in Figure 3A, the percentages of splenic CD19⁺ B cells in lymphocytes were comparable in WT and Fc γ RIIb^{232T/T} mice. However, the percentage of NP⁺CD19⁺ B cells was substantially increased in

Fc γ RIIb^{232T/T} mice compared to WT mice after secondary immunization. Similarly, the percentage of splenic CD19⁺CD138⁺ PCs in Fc γ RIIb^{232T/T} mice was not different from that in WT mice, but the percentage of NP⁺CD19⁺CD138⁺ PCs was significantly increased in Fc γ RIIb^{232T/T} mice ($P < 0.001$) (Figure 3B).

We next used ELISpot assays to quantify the numbers of splenic NP⁺ PCs. Consistent with an increased level of circulating NP₃₀+ IgG, a greater number of NP₃₀+IgG+ PCs was detected in Fc γ RIIb^{232T/T} mice than in WT mice ($P < 0.05$) (Figure 3C). Further analysis of splenic NP⁺IgG+ PCs revealed no significant

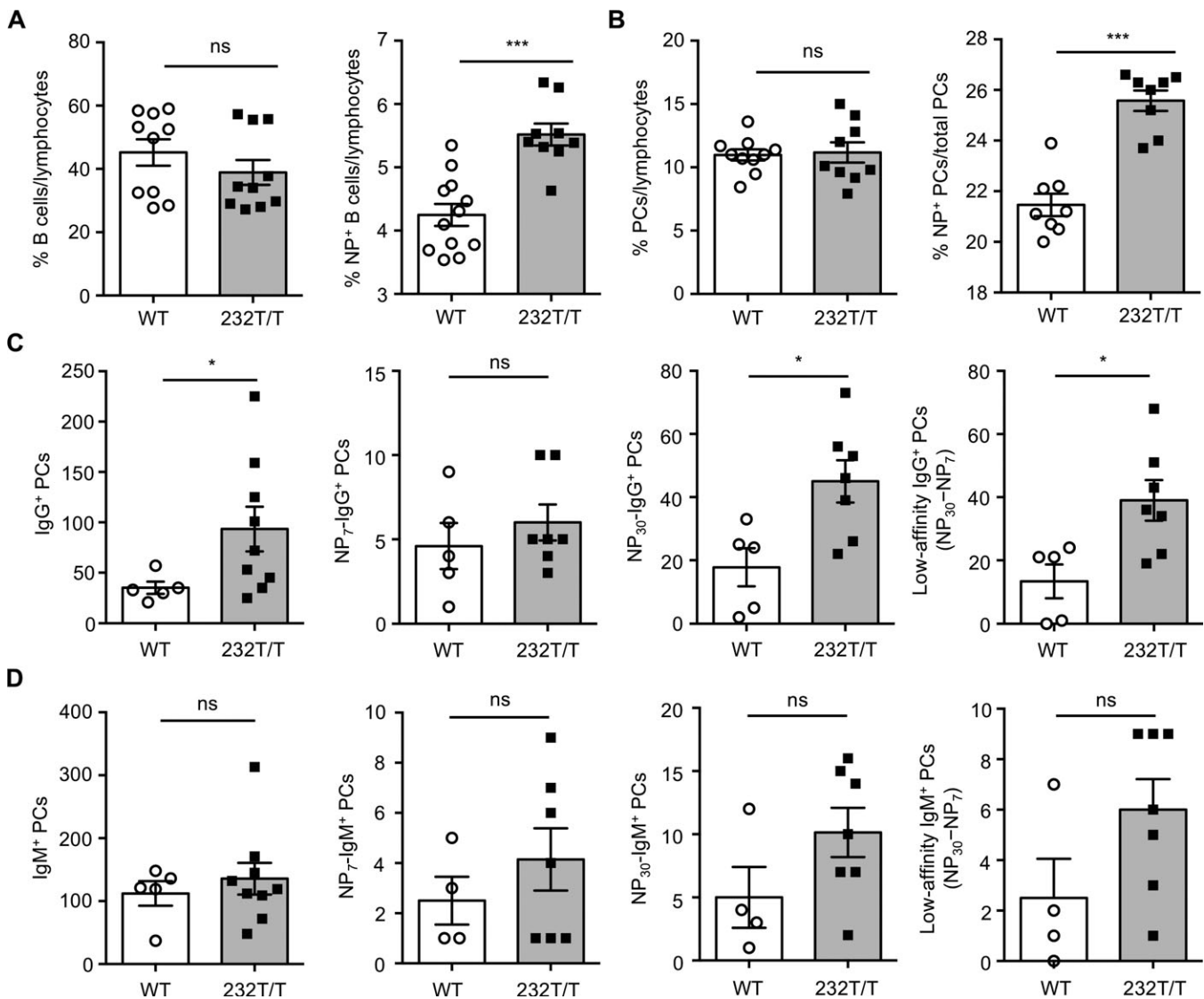


Figure 3. Increased frequency of low-affinity NP+IgG+ plasma cells (PCs) in the spleen in Fc γ receptor IIb (Fc γ RIIb)^{232T/T} mice after secondary immunization. **A and B,** Percentages of CD19+ B cells ($P = 0.2846$) and NP+CD19+ B cells ($P = 0.0007$) (**A**) and percentages of CD19+CD138+ PCs ($P = 0.8432$) and NP+CD19+CD138+ PCs ($P = 0.0009$) (**B**) in splenic lymphocytes from wild-type (WT) mice and Fc γ RIIb^{232T/T} mice on day 35, analyzed by flow cytometry. **C,** Splenic total IgG+ PCs ($P = 0.0315$), high-affinity NP₇-specific IgG+ PCs ($P = 0.4318$), total NP₃₀-specific IgG+ PCs ($P = 0.0168$), and low-affinity NP+IgG+ (NP₃₀ minus NP₇) PCs ($P = 0.0159$) in WT mice and Fc γ RIIb^{232T/T} mice on day 35, determined using enzyme-linked immunospot assays (using 6×10^3 cells to detect total PCs and 2.4×10^4 cells to detect NP+ PCs). **D,** Numbers of total IgM+ PCs ($P = 0.5412$), NP₇-specific IgM+ PCs ($P = 0.355$), NP₃₀-specific IgM+ PCs ($P = 0.116$), and low-affinity NP+IgM+ (NP₃₀ minus NP₇) PCs ($P = 0.0864$) in WT mice and Fc γ RIIb^{232T/T} mice. Symbols represent individual mice; bars show the mean \pm SEM ($n = 8$ – 12 WT mice and 8 – 10 Fc γ RIIb^{232T/T} mice in **A** and **B**; $n = 5$ WT mice and 7 – 9 Fc γ RIIb^{232T/T} mice in **C**; $n = 4$ – 5 WT mice and 7 – 9 Fc γ RIIb^{232T/T} mice in **D**). * = $P < 0.05$; *** = $P < 0.001$. NS = not significant.

differences in the numbers of high-affinity NP₇+ PCs between WT and Fc γ RIIb^{232T/T} mice. In contrast, compared to WT mice, the numbers of low-affinity IgG+ PCs (NP₃₀+ PCs minus NP₇+ PCs) increased ~ 3 -fold in Fc γ RIIb^{232T/T} mice ($P < 0.05$) (Figure 3C). These differences were not observed when the numbers of NP+IgM+ PCs were compared between WT and Fc γ RIIb^{232T/T} mice (Figure 3D), suggesting a specific IgG-associated effect

through Fc γ RIIb. Of interest, we found that the numbers of low-affinity NP+IgG+ PCs were also significantly increased in heterozygous Fc γ RIIb-232T mice compared to WT mice (see Supplementary Figure 2, available on the *Arthritis & Rheumatology* web site at <http://onlinelibrary.wiley.com/doi/10.1002/art.40555/abstract>). These findings suggest that Fc γ RIIb-232T might impede recruitment of sufficient amounts of WT receptors to reach the threshold

required for efficient induction for apoptosis. Consistent with this notion, we previously demonstrated that Fc γ RIIb-mediated apoptosis is dependent on the signal strength transduced from the receptor oligomers (5).

Tfh cell number and function in switching IgG isotypes are not altered in Fc γ RIIb^{232T/T} mice. Because the generation of PCs is influenced by Tfh (CD4+B220+PD-

1+ICOS+) cells, which provide help, e.g., interleukin-21, to GC B cells to further their differentiation into PCs and to class-switch IgG isotypes (32,33), we examined the numbers of splenic Tfh cells to determine their contributions to the increase in NP+IgG+ PCs in Fc γ RIIb^{232T/T} mice. As shown in Figure 4A, the numbers of Tfh cells were comparable between immunized WT and Fc γ RIIb^{232T/T}

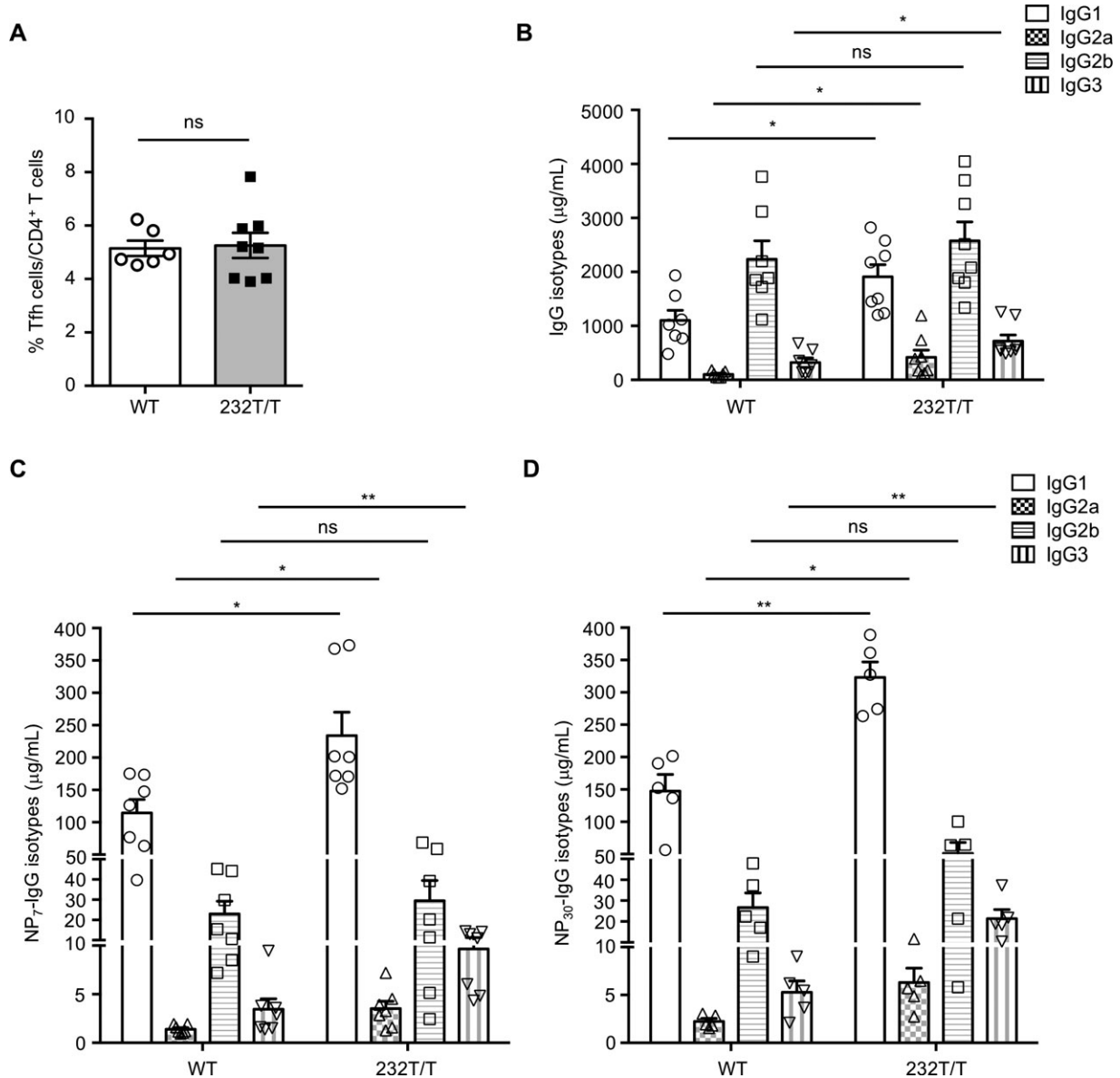


Figure 4. Splenic follicular helper T (Tfh) cell numbers and serum titers of class-switched NP+ IgG isotypes in wild-type (WT) and Fc γ receptor IIb (Fc γ RIIb)^{232T/T} mice. **A**, Percentages of Tfh cells (CD4+B220+ programmed death 1-positive inducible costimulator-positive) in splenic T cells in WT mice and Fc γ RIIb^{232T/T} mice on day 35 ($P = 0.8622$). **B**, Serum concentrations of IgG1 ($P = 0.0098$), IgG2a ($P = 0.0076$), IgG2b ($P = 0.9813$), and IgG3 ($P = 0.045$) in immunized WT mice and Fc γ RIIb^{232T/T} mice. **C** and **D**, Serum levels of high-affinity NP₇-specific IgG isotypes (IgG1 [$P = 0.0137$], IgG2a [$P = 0.0178$], IgG2b [$P = 0.5956$], and IgG3 [$P = 0.0091$]) (**C**) and total NP₃₀-specific IgG isotypes (IgG1 [$P = 0.0011$], IgG2a [$P = 0.0283$], IgG2b [$P = 0.217$], and IgG3 [$P = 0.0079$]) (**D**) in WT and Fc γ RIIb^{232T/T} mice. Symbols represent individual mice; bars show the mean \pm SEM ($n = 6$ WT mice and 8 Fc γ RIIb^{232T/T} mice in **A**; $n = 7$ WT mice and 8 Fc γ RIIb^{232T/T} mice in **B**; $n = 5-7$ mice per group in **C** and **D**). * = $P < 0.05$; ** = $P < 0.01$. NS = not significant.

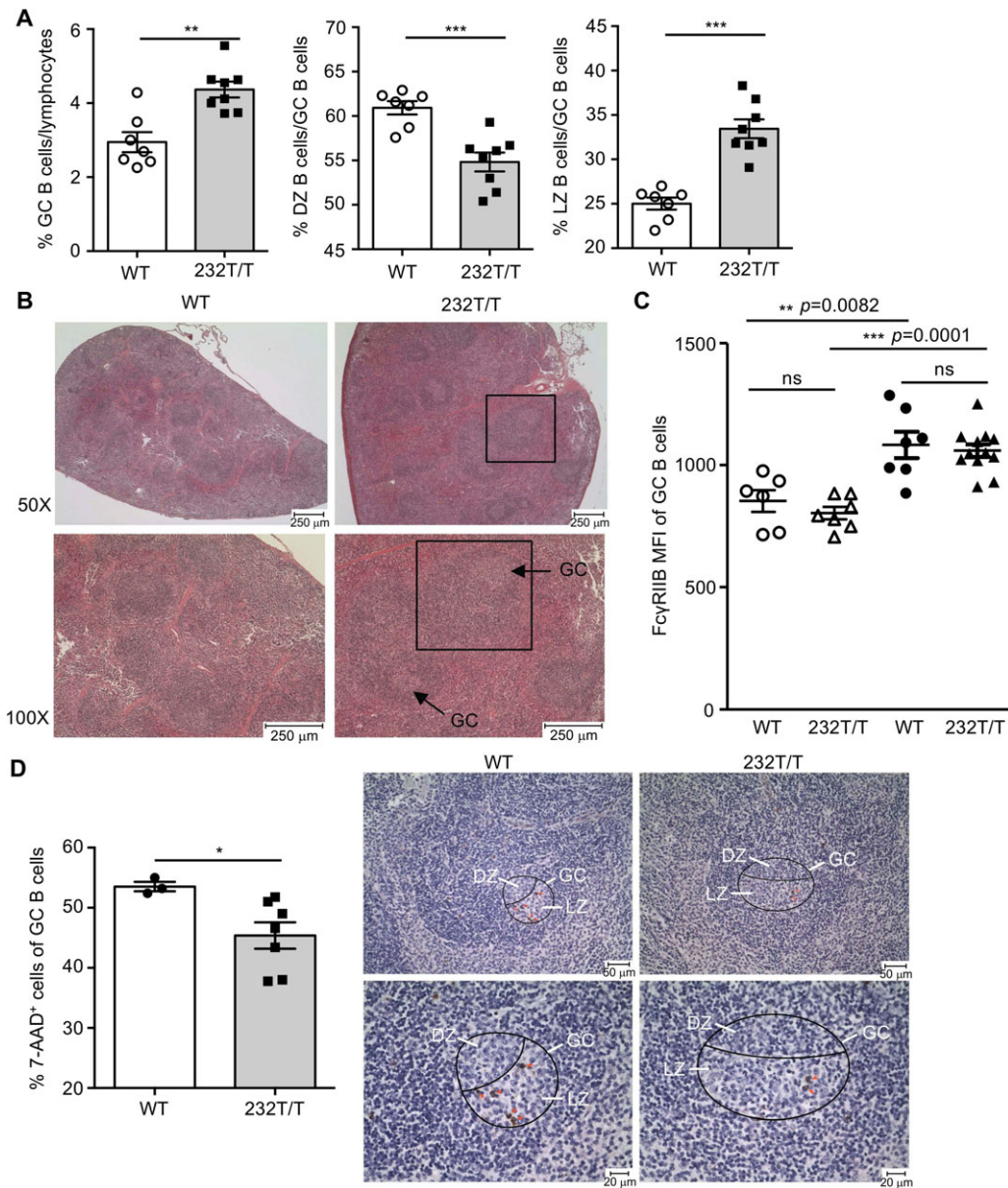


Figure 5. Increased numbers of light zone (LZ) germinal center (GC) B cells and reduced numbers of apoptotic GC B cells in Fcγ receptor IIb (FcγRIIb)^{232T/T} mice after secondary immunization. **A**, Percentages of splenic CD19+GL-7+ GC B cells ($P = 0.0011$), dark zone (DZ) NP+ GC B cells ($P = 0.0005$), and light zone NP+ GC B cells ($P = 0.0002$) in WT mice and FcγRIIb^{232T/T} mice. Symbols represent individual mice; bars show the mean \pm SEM ($n = 7$ WT mice and 8 FcγRIIb^{232T/T} mice). **B**, Representative splenic sections from WT and FcγRIIb^{232T/T} mice showing the size of GCs. Bottom panels are higher-magnification views of the top panels. The boxed areas show follicles. **C**, Surface expression levels of FcγRIIb on GC B cells in age-matched nonimmunized WT and FcγRIIb^{232T/T} mice (open symbols) ($P = 0.3613$) and immunized WT and FcγRIIb^{232T/T} mice on day 35 (solid symbols) ($P = 0.7026$). There was a significant difference in expression of FcγRIIb in nonimmunized WT mice versus immunized WT mice ($P = 0.0082$) and in nonimmunized FcγRIIb^{232T/T} mice versus immunized FcγRIIb^{232T/T} mice ($P = 0.0001$). Symbols represent individual mice; horizontal and vertical lines show the mean \pm SEM ($n = 6$ nonimmunized WT mice, 7 nonimmunized FcγRIIb^{232T/T} mice, 7 immunized WT mice, and 11 immunized FcγRIIb^{232T/T} mice). MFI = mean fluorescence intensity. **D**, Left, Percentages of 7-aminoactinomycin D (7-AAD)+GL-7+ GC B cells in WT mice and FcγRIIb^{232T/T} mice ($P = 0.0484$). Symbols represent individual mice; bars show the mean \pm SEM ($n = 3$ WT mice and 7 FcγRIIb^{232T/T} mice). Right, Staining for active caspase 3 to detect apoptotic GC B cells in the light zone of GCs (encircled areas) in splenic sections from WT and FcγRIIb^{232T/T} mice. * = $P < 0.05$; ** = $P < 0.01$; *** = $P < 0.001$. NS = not significant.

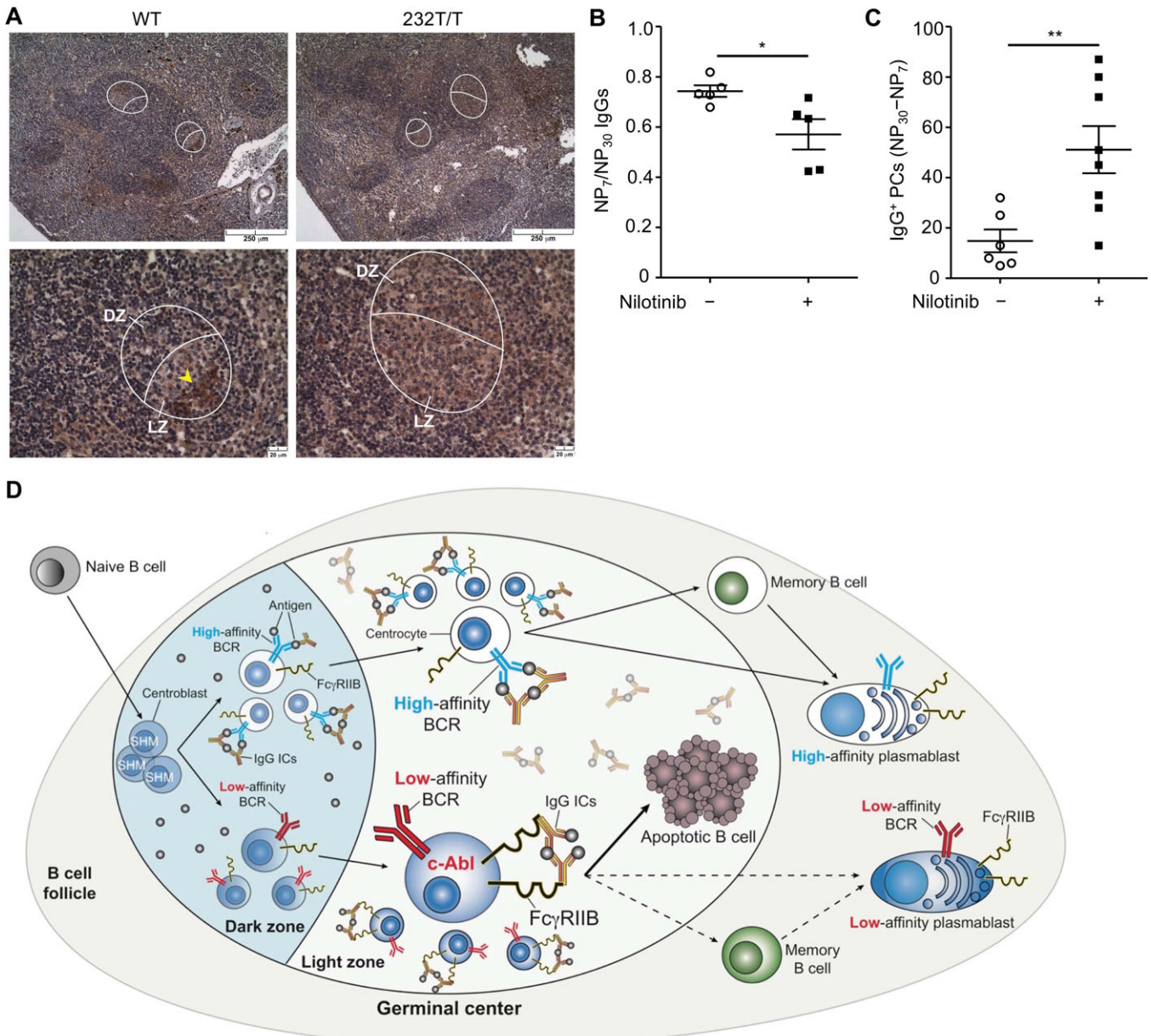


Figure 6. Association of reduced c-Abl activation with retention of low-affinity germinal center (GC) B cells in mice after secondary immunization. **A**, Reduced staining of phospho-c-Abl (Y245)+ GC B cells (arrowhead) in Fc γ receptor IIb (Fc γ R1IB)^{232T/T} mice compared to wild-type (WT) mice. Female WT mice (7–8 weeks old) were immunized as described in Figure 1B. Mice were treated with either vehicle or nilotinib (2 mg/kg/day) on days 7–9 after the second immunization. Encircled areas show GCs. Bottom panels show higher-magnification views of the top panels. **B** and **C**, Ratio of NP₇ to NP₃₀ serum IgG ($P = 0.0283$) (**B**) and number of low-affinity NP+IgG+ (NP₃₀ minus NP₇) plasma cells in splenocytes (2.4×10^4) ($P = 0.0087$) in vehicle-treated WT mice and nilotinib-treated WT mice. Symbols represent individual mice; horizontal and vertical lines show the mean \pm SEM ($n = 5$ –6 vehicle-treated mice and 5–8 nilotinib-treated mice). * = $P < 0.05$; ** = $P < 0.01$. **D**, Illustration of the crucial role of Fc γ R1IB in the negative selection of low-affinity GC B cells via c-Abl in the light zone of GCs in response to IgG immune complexes (ICs) in secondary immunization in WT mice (solid lines). Broken lines represent Fc γ R1IB^{232T/T} mice. BCR = B cell receptor; SHM = somatic hypermutation.

mice ($P = 0.8622$) despite an increased number of NP+ PCs in Fc γ R1IB^{232T/T} mice (Figure 3). Consistent with increased serum levels of total IgG in Fc γ R1IB^{232T/T} mice

(Figure 2A), the serum concentrations of IgG1, IgG2a, and IgG3 isotypes were all significantly higher in immunized Fc γ R1IB^{232T/T} mice than WT mice ($P < 0.05$)

(Figure 4B). Similarly, the serum levels of high-affinity (NP₇)-specific and total NP+ (NP₃₀)-specific IgG isotypes remained higher in FcγRIIb^{232T/T} mice than in WT mice (Figures 4C and D).

Reduced apoptosis of B cells in GC light zones of immunized FcγRIIb^{232T/T} mice. To further delineate the abnormality of GC response in FcγRIIb^{232T/T} mice, we quantified NP+CD19+GL-7+ GC B cells and found that FcγRIIb^{232T/T} mice exhibited more splenic NP+ GC B cells than WT mice (Figure 5A). When GC dark zone (CD86^{low}CXCR4^{high}) and light zone (CD86^{high}CXCR4^{low}) B cells were analyzed and compared, we found a decreased percentage of GC dark zone B cells ($P < 0.001$) (Figure 5A) but an increased percentage of GC light zone B cells ($P < 0.001$) (Figure 5A) in FcγRIIb^{232T/T} mice. Moreover, we detected an increase in the size of GCs in splenic sections from immunized FcγRIIb^{232T/T} mice (Figure 5B). It has been shown that the surface expression of FcγRIIb in GC B cells is up-regulated in normal mice (16). We examined the FcγRIIb expression levels in GC B cells and found no significant differences in FcγRIIb expression between WT and FcγRIIb^{232T/T} mice either before or after immunization (Figure 5C). Because clonal selection of GC B cells occurs primarily in the light zone of GCs (17–22), we next investigated the apoptosis of GC B cells to determine the extent of negative selection of low-affinity B cells after secondary immunization. Consistent with an increase in GC B cell numbers in FcγRIIb^{232T/T} mice, the percentage of dead GC B cells was significantly decreased in these mice ($P < 0.05$) (Figure 5D). Significantly fewer apoptotic GC B cells, which were stained by active caspase 3 mAb, were detected in FcγRIIb^{232T/T} mice after secondary immunization (Figure 5D).

Blocking c-Abl activity in WT mice during clonal selection recapitulates the GC phenotype of FcγRIIb^{232T/T} mice. Because FcγRIIb is known to mediate apoptosis via c-Abl kinase in response to IgG ICs in B cells (5), we investigated the expression of active c-Abl (p-Y245) proteins in GC B cells. In WT mice, phospho-c-Abl proteins were readily detectable and mainly localized in the light zone of GCs, where affinity maturation and clonal selection occur. In contrast, the levels of phospho-c-Abl proteins were substantially decreased in the GCs of FcγRIIb^{232T/T} mice (Figure 6A). It has been reported that the apoptosis of GC B cells peaks during days 7–9 after secondary immunization (34). Thus, to determine whether c-Abl activity is crucial for FcγRIIb to negatively regulate GC B cells, we treated WT mice with nilotinib (2 mg/kg/day) to block c-Abl kinase activity during the peak period when GC B cells undergo apoptosis for selection after secondary immunization. Indeed, the serum titers of NP+ IgG displayed reduced affinity maturation

in nilotinib-treated mice ($P < 0.05$) (Figure 6B). Moreover, the number of low-affinity NP+IgG+ PCs (NP₃₀ PCs minus NP₇ PCs) was significantly increased after c-Abl kinase activity was blocked in WT mice ($P < 0.01$) (Figure 6C). Thus, the findings in antibodies produced from nilotinib-treated WT mice are reminiscent of the GC defect observed in FcγRIIb^{232T/T} mice after secondary immunization (Figures 2 and 3).

DISCUSSION

In this study, we showed for the first time that compromised inhibitory activity of FcγRIIb-232T proteins results in insufficient deletion of low-affinity antigen-specific GC B cells and reduces affinity maturation in clonal selection. Consequently, the resultant increase in low-affinity antigen-specific GC B cells leads to a corresponding increase in low-affinity antigen-specific IgG in circulation in FcγRIIb^{232T/T} mice (Figures 2 and 3). Compared to WT mice, the number of GC light zone B cells was increased in FcγRIIb^{232T/T} mice due to a decrease in the apoptosis of GC B cells and in the phosphorylation of c-Abl proteins (Figures 5 and 6). Furthermore, administration of nilotinib to WT mice to block c-Abl kinase activity at the peak of apoptosis of GC B cells in clonal selection resulted in reduced affinity maturation reminiscent of the phenotype of immunized FcγRIIb^{232T/T} mice. The involvement of c-Abl in the clonal selection of GC B cells is a novel and important finding. The newly identified, crucial role of FcγRIIb in regulating the stringency of affinity maturation by triggering apoptosis to delete low-affinity GC B cells via c-Abl is illustrated in Figure 6D.

Because FcγRIIb^{232T/T} mice display a higher serum level of high-affinity NP-specific IgG, the reduced inhibition of FcγRIIb-232T on BCRs might have the potential to promote the proliferation of GC B cells. Indeed, numbers of GC B cells increased in FcγRIIb^{232T/T} mice after secondary immunization (Figure 5A). Nevertheless, the increased number of B cells was largely due to an increase in low-affinity B cells, since no increase in high-affinity IgG+ PCs was observed in FcγRIIb^{232T/T} mice (Figure 3). This leads us to conclude that the retention of low-affinity B cells is more a consequence of insufficient apoptosis rather than insufficient inhibition of proliferation of GC B cells in FcγRIIb^{232T/T} mice. In addition, because low-affinity B cells are intrinsically less competitive than high-affinity cells for antigen stimulation, the increased survival of low-affinity FcγRIIb^{232T/T} GC B cells is positively associated with reduced apoptosis. One important caveat is that low-affinity antigen-specific GC B cells may have a chance to undergo further affinity maturation when the competition with high-affinity B cells becomes reduced in late

GCs (35). However, in the persistence of Fc γ RIIb-232T dysfunction, repeated immunization generates a new pool of low-affinity B cells, which normally should have been deleted. Consistent with this finding, the serum level of low-affinity antigen-specific IgG and the number of IgG+ PCs remained significantly increased after secondary immunization in Fc γ RIIb^{232T/T} mice (Figures 2 and 3).

These findings raise the possibility of undesired consequences of enhanced immune response due to the presence of the Fc γ RIIb-232T allele. For example, low-affinity memory B cells might persist in peripheral lymphoid organs, and low-affinity PCs emigrated from GCs into circulation might be able to become long-term residents in the bone marrow to secrete low-affinity antibodies (36). An additional caveat is that because serum NP+ IgG display increasing affinity maturation in WT mice over time but remain reduced in Fc γ RIIb^{232T/T} mice after primary immunization, the contribution of extrafollicular response to influence the outcome of low-affinity B cells is likely limited (Supplementary Figure 3, available on the *Arthritis & Rheumatology* web site at <http://onlinelibrary.wiley.com/doi/10.1002/art.40555/abstract>).

Consistent with previous findings in living cells (14,15), Fc γ RIIb-I232T proteins appear to form small raft-associated clusters rather than coalesced caps for signal amplification as compared to receptors in WT mice at 30–60 minutes (see Supplementary Figure 1, available on the *Arthritis & Rheumatology* web site at <http://onlinelibrary.wiley.com/doi/10.1002/art.40555/abstract>). The resultant diminished recruitment of SHIP to Fc γ RIIb-232T therefore can account for reduced inhibition on B cells in response to IgG ICs. However, mice deficient in the *Ship* gene show no differences from WT mice in antibody production after immunization with a T cell-dependent antigen (37). Nevertheless, when the *Ship* gene is specifically deleted in B cells, they are indeed more sensitive to antigen activation than WT cells in vitro (38).

Surprisingly, the number of NP+ GC B cells and the serum level of NP+ IgG decreased markedly after NP-CGG immunization. It appears that hyperactive BCR signaling in SHIP-deficient GC B cells directly induces apoptosis of both low- and high-affinity B cells (38). Thus, a tightly regulated balance between Fc γ RIIb/SHIP and Fc γ RIIb/c-Abl pathways in response to IgG ICs is crucial for normal outcome of GC reaction. Consistent with this notion, an increased sensitivity to Fc γ RIIb-dependent apoptosis might contribute in part to the GC phenotype in mice with SHIP deficiency in B cells. Indeed, loss of SHIP in DT40 B cells enhances Fc γ RIIb-induced apoptosis (9). We previously showed that apoptosis of B cells induced by Fc γ RIIb is dependent on c-Abl, but independent of SHIP, suggesting a decisive role of c-Abl when activated (5).

In the GC, low-affinity B cells are outcompeted by high-affinity B cells for antigen stimulation and Tfh cell help, thereby lacking survival advantages (39,40). In the present study, we provided evidence of a new role of the Fc γ RIIb/c-Abl signaling pathway to participate in the negative selection of low-affinity B cells. Consistent with our findings, enhancing survival of GC B cells by overexpression of the *Bcl-x_L* gene in mice results in reduced affinity maturation (41). Similarly, mice overexpressing *Bcl-2* show decreased negative selection of GC B cells (42,43). These findings indicate that enhanced BCR signaling can increase the survival of low-affinity B cells to avoid negative selection. Whether these low-affinity B cells might have overcome the apoptotic induction from Fc γ RIIb to escape deletion is of interest for future studies. Meanwhile, it has been demonstrated that low-affinity autoreactive B cells are more sensitive to CpG double-stranded DNA-induced differentiation into PCs than high-affinity B cells (44,45). Thus, low-affinity autoreactive B cells are able to efficiently expand independent of antigen stimulation if they can escape from elimination in GCs. Because autoreactive B cells are routinely generated in response to a foreign antigen in normal mice, e.g., resulting from host immune response against pathogens (46), low-affinity autoreactive B cells, which are likely generated from time to time, need to be deleted when they emerge in GCs to prevent autoimmunity.

Our findings indicate that in Fc γ RIIb-232T allele carriers, the persistent presence of low-affinity B cells and especially PCs may gradually become a key contributor that puts them at risk of developing autoimmune diseases over time. Reduced surface expression levels of WT Fc γ RIIb in the B cells of SLE patients may result in susceptibility to the presence of low-affinity B cells (18–20). Accordingly, because transgenic mice overexpressing *Fcgr2b* in B cells exhibit reduced SLE disease severity (47), it will be of interest to investigate whether regimens that up-regulate the surface expression level of Fc γ RIIb-232T proteins to enhance their inhibition can restore competency to negatively regulate low-affinity GC B cells for therapeutic exploitation.

ACKNOWLEDGMENTS

We thank Miss Yu-Syuan You and Mr. Tsung-Chih Tseng for excellent technical assistance. We acknowledge Dr. Shu-Wha Lin for the technical assistance and service provided by the Gene Knockout Mouse Core of the NTU Center for Genomic Medicine, College of Medicine, National Taiwan University. We also appreciate the services provided by the staff of the First Core Laboratory at the College of Medicine, National Taiwan University and the RCF7 Laboratory of the Department of Medical Research at National Taiwan University Hospital.

AUTHOR CONTRIBUTIONS

All authors were involved in drafting the article or revising it critically for important intellectual content, and all authors approved the final version to be published. Dr. Tzeng had full access to all of the data in the study and takes responsibility for the integrity of the data and the accuracy of the data analysis.

Study conception and design. Jhou, Tzeng.

Acquisition of data. Jhou, Yu, Hwai, C.-S. Chen, Tzeng.

Analysis and interpretation of data. Jhou, Hwai, P.-L. Chen, Tzeng.

REFERENCES

- Daeron M. Fc receptors as adaptive immunoreceptors. *Curr Top Microbiol Immunol* 2014;382:131–64.
- Espéli M, Smith KG, Clatworthy MR. FcγRIIB and autoimmunity. *Immunol Rev* 2016;269:194–211.
- Bolland S, Ravetch JV. Spontaneous autoimmune disease in FcγRIIB-deficient mice results from strain-specific epistasis. *Immunity* 2000;13:277–85.
- Tiller T, Kofer J, Kreschel C, Busse CE, Riebel S, Wickert S, et al. Development of self-reactive germinal center B cells and plasma cells in autoimmune FcγRIIB-deficient mice. *J Exp Med* 2010;207:2767–78.
- Tzeng SJ, Bolland S, Inabe K, Kurosaki T, Pierce SK. The B cell inhibitory Fc receptor triggers apoptosis by a novel c-Abl family kinase-dependent pathway. *J Biol Chem* 2005;280:35247–54.
- Chacko GW, Tridandapani S, Damen JE, Liu L, Krystal G, Coggeshall KM. Negative signaling in B lymphocytes induces tyrosine phosphorylation of the 145-kDa inositol polyphosphate 5-phosphatase, SHIP. *J Immunol* 1996;157:2234–8.
- D'Ambrosio D, Fong DC, Cambier JC. The SHIP phosphatase becomes associated with FcγRIIB1 and is tyrosine phosphorylated during 'negative' signaling. *Immunol Lett* 1996;54:77–82.
- Ono M, Bolland S, Tempst P, Ravetch JV. Role of the inositol phosphatase SHIP in negative regulation of the immune system by the receptor FcγRIIB. *Nature* 1996;383:263–6.
- Pearse RN, Kawabe T, Bolland S, Guinamard R, Kurosaki T, Ravetch JV. SHIP recruitment attenuates FcγRIIB-induced B cell apoptosis. *Immunity* 1999;10:753–60.
- Siriboonrit U, Tsuchiya N, Sirikong M, Kyogoku C, Bejrachandra S, Suthipinittharm P, et al. Association of Fcγ receptor IIb and IIb polymorphisms with susceptibility to systemic lupus erythematosus in Thais. *Tissue Antigens* 2003;61:374–83.
- Chen JY, Wang CM, Ma CC, Luo SF, Edberg JC, Kimberly RP, et al. Association of a transmembrane polymorphism of Fcγ receptor IIb (FCGR2B) with systemic lupus erythematosus in Taiwanese patients. *Arthritis Rheum* 2006;54:3908–17.
- Willcocks LC, Carr EJ, Niederer HA, Rayner TF, Williams TN, Yang W, et al. A defuncting polymorphism in FCGR2B is associated with protection against malaria but susceptibility to systemic lupus erythematosus. *Proc Natl Acad Sci U S A* 2010;107:7881–5.
- Kono H, Kyogoku C, Suzuki T, Tsuchiya N, Honda H, Yamamoto K, et al. FcγRIIB Ile232Thr transmembrane polymorphism associated with human systemic lupus erythematosus decreases affinity to lipid rafts and attenuates inhibitory effects on B cell receptor signaling. *Hum Mol Genet* 2005;14:2881–92.
- Sohn HW, Pierce SK, Tzeng SJ. Live cell imaging reveals that the inhibitory FcγRIIB destabilizes B cell receptor membrane-lipid interactions and blocks immune synapse formation. *J Immunol* 2008;180:793–9.
- Xu L, Xia M, Guo J, Sun X, Li H, Xu C, et al. Impairment on the lateral mobility induced by structural changes underlies the functional deficiency of the lupus-associated polymorphism FcγRIIB-T232. *J Exp Med* 2016;213:2707–27.
- Clatworthy MR, Willcocks L, Urban B, Langhorne J, Williams TN, Peshu N, et al. Systemic lupus erythematosus-associated defects in the inhibitory receptor FcγRIIB reduce susceptibility to malaria. *Proc Natl Acad Sci U S A* 2007;104:7169–74.
- Waisberg M, Tarasenko T, Vickers BK, Scott BL, Willcocks LC, Molina-Cruz A, et al. Genetic susceptibility to systemic lupus erythematosus protects against cerebral malaria in mice. *Proc Natl Acad Sci U S A* 2011;108:1122–7.
- Mackay M, Stanevsky A, Wang T, Aranow C, Li M, Koenig S, et al. Selective dysregulation of the FcγIIB receptor on memory B cells in SLE. *J Exp Med* 2006;203:2157–64.
- Su K, Yang H, Li X, Li X, Gibson AW, Cafardi JM, et al. Expression profile of FcγRIIB on leukocytes and its dysregulation in systemic lupus erythematosus. *J Immunol* 2007;178:3272–80.
- Isaák A, Gergely P Jr, Szekeres Z, Prechl J, Poór G, Erdei A, et al. Physiological up-regulation of inhibitory receptors FcγRII and CR1 on memory B cells is lacking in SLE patients. *Int Immunol* 2008;20:185–92.
- Rahman ZS, Manser T. Failed up-regulation of the inhibitory IgG Fc receptor FcγRIIB on germinal center B cells in autoimmune-prone mice is not associated with deletion polymorphisms in the promoter region of the FcγRIIB gene. *J Immunol* 2005;175:1440–9.
- MacLennan IC, Gray D. Antigen-driven selection of virgin and memory B cells. *Immunol Rev* 1986;91:61–85.
- French DL, Laskov R, Scharff MD. The role of somatic hypermutation in the generation of antibody diversity. *Science* 1989;244:1152–7.
- Gitlin AD, Shulman Z, Nussenzweig MC. Clonal selection in the germinal centre by regulated proliferation and hypermutation. *Nature* 2014;509:637–40.
- MacLennan IC. Germinal centers. *Annu Rev Immunol* 1994;12:117–39.
- De Silva NS, Klein U. Dynamics of B cells in germinal centres. *Nat Rev Immunol* 2015;15:137–48.
- Goins CL, Chappell CP, Shashidharamurthy R, Selvaraj P, Jacob J. Immune complex-mediated enhancement of secondary antibody responses. *J Immunol* 2010;184:6293–8.
- Qin D, Wu J, Vora KA, Ravetch JV, Szakal AK, Manser T, et al. Fcγ receptor IIb on follicular dendritic cells regulates the B cell recall response. *J Immunol* 2000;164:6268–75.
- Tzeng SJ. The isolation, differentiation, and quantification of human antibody-secreting B cells from blood: ELISpot as a functional readout of humoral immunity. *J Vis Exp* 2016;118:e54582.
- Tzeng SJ, Li WY, Wang HY. FcγRIIB mediates antigen-independent inhibition on human B lymphocytes through Btk and p38 MAPK. *J Biomed Sci* 2015;22:87–98.
- Dominguez-Sola D, Victora GD, Ying CY, Phan RT, Saito M, Nussenzweig MC, et al. The proto-oncogene MYC is required for selection in the germinal center and cyclic reentry. *Nat Immunol* 2012;13:1083–91.
- Li H, Durbin R. Fast and accurate short read alignment with Burrows-Wheeler transform. *Bioinformatics* 2009;25:1754–60.
- Li H, Handsaker B, Wysoker A, Fennell T, Ruan J, Homer N, et al. The sequence alignment/map format and SAMtools. *Bioinformatics* 2009;25:2078–9.
- Saitoh HA, Maeda K, Yamakawa M. In situ observation of germinal center cell apoptosis during a secondary immune response. *J Clin Exp Hematol* 2006;46:73–82.
- Dal Porto JM, Haberman AM, Kelsoe G, Shlomchik MJ. Very low affinity B cells form germinal centers, become memory B cells, and participate in secondary immune responses when higher affinity competition is reduced. *J Exp Med* 2002;195:1215–21.
- Jacob J, Kelsoe G. In situ studies of the primary immune response to (4-hydroxy-3-nitrophenyl)acetyl. Part II. A common clonal origin for periarteriolar lymphoid sheath-associated foci and germinal centers. *J Exp Med* 1992;176:679–87.
- Helgason CD, Kalberer CP, Damen JE, Chappel SM, Pineault N, Krystal G, et al. A dual role for Src homology 2 domain-containing inositol-5-phosphatase (SHIP) in immunity: aberrant development

- and enhanced function of B lymphocytes in *shp*^{-/-} mice. *J Exp Med* 2000;191:781–94.
38. Leung WH, Tarasenko T, Biesova Z, Kole H, Walsh ER, Bolland S. Aberrant antibody affinity selection in SHIP-deficient B cells. *Eur J Immunol* 2013;43:371–81.
 39. Shulman Z, Gitlin AD, Targ S, Jankovic M, Pasqual G, Nussenzweig MC, et al. T follicular helper cell dynamics in germinal centers. *Science* 2013;341:673–7.
 40. Shulman Z, Gitlin AD, Weinstein JS, Lainez B, Esplugues E, Flavell RA, et al. Dynamic signaling by T follicular helper cells during germinal center B cell selection. *Science* 2014;345:1058–62.
 41. Takahashi Y, Cerasoli DM, Dal Porto JM, Shimoda M, Freund R, Fang W, et al. Relaxed negative selection in germinal centers and impaired affinity maturation in *bcl-xL* transgenic mice. *J Exp Med* 1999;190:399–410.
 42. Hande S, Notidis E, Manser T. Bcl-2 obstructs negative selection of autoreactive, hypermutated antibody V regions during memory B cell development. *Immunity* 1998;8:189–98.
 43. Smith KG, Light A, O'Reilly LA, Ang SM, Strasser A, Tarlinton D. Bcl-2 transgene expression inhibits apoptosis in the germinal center and reveals differences in the selection of memory B cells and bone marrow antibody-forming cells. *J Exp Med* 2000;191:475–84.
 44. Rui L, Vinuesa CG, Blasioli J, Goodnow CC. Resistance to CpG DNA-induced autoimmunity through tolerogenic B cell antigen receptor ERK signaling. *Nat Immunol* 2003;4:594–600.
 45. Viglianti GA, Lau CM, Hanley TM, Miko BA, Shlomchik MJ, Marshak-Rothstein A. Activation of autoreactive B cells by CpG dsDNA. *Immunity* 2003;19:837.
 46. Ray SK, Putterman C, Diamond B. Pathogenic autoantibodies are routinely generated during the response to foreign antigen: a paradigm for autoimmune disease. *Proc Natl Acad Sci U S A* 1996;93:2019–24.
 47. Brownlie RJ, Lawlor KE, Niederer HA, Cutler AJ, Xiang Z, Clatworthy MR, et al. Distinct cell-specific control of autoimmunity and infection by Fc γ RIIb. *J Exp Med* 2008;205:883–95.